Available online at www.sciencedirect.com
SCIENCE DIRECT®
PERGAMON
Solid-State Electronics 47 (2003) 1369–1377
SOLID-STATE ELECTRONICS
www.elsevier.com/locate/sse

Accessing transmission-mode dispersion in super-prisms

Y. Du, A.F.J. Levi *

Department of Electrical Engineering, University of Southern California, KAP 132, Los Angeles, CA 90089-2533, USA

Received 18 November 2002; received in revised form 2 December 2002; accepted 3 January 2003

Abstract

Breaking the symmetry of a photonic crystal allows external access to large near band-edge optical dispersion and exploitation of super-prism effects in a transmission mode device. Acceptable performance is obtained by spatially varying the scattering strength of the dielectric structure according to a modified exponential function. However, our analysis shows that useful devices operating with incident wavelength near 1550 nm will require fabrication tolerances on the scale of less than 10 nm.

Keywords: Super-prism; Impedance matching; Photonic crystal; Scattering matrix

1. Introduction

Since Ohtaka [1] analyzed dispersion in three-dimensional periodic dielectric structures, there has been interest in exploiting strong near band-gap photon refraction and dispersion of nano-fabricated periodic dielectrics or photonic crystals (PCs). Potential applications include super-prisms [2,3] in which the usual underlying concept is exploitation of strongly dispersive Bloch modes near a band-edge.

Typically, the super-prism idea is discussed for the limiting case of an infinite sized PC. However, in practical, finite sized PCs, resonant effects can dominate and complicate analysis. Unlike electromagnetic wave propagation in a homogeneous medium, the light beam can be scattered into different Bloch modes of the PC and propagate along different directions [4]. Snell's law as applied to effective medium theory is not valid for near band-edge incident radiation in finite PCs. Large dispersion and resonant interference effects dominate electromagnetic energy flow through the dielectric structure.

As a starting point we consider electromagnetic wave propagation using the conventional wave packet description [5]. The group velocity in a medium with dispersion $\omega(\mathbf{k})$ is

$$\mathbf{v}_g = \nabla_{\mathbf{k}}\omega = \frac{\mathbf{S}}{U} - \left(\frac{\partial \mu_{\mathbf{k}}}{\partial \mathbf{k}}\right)\cdot\frac{\omega\mathbf{H}\cdot\mathbf{H}}{U} - \left(\frac{\partial \varepsilon_{\mathbf{k}}}{\partial \mathbf{k}}\right)\cdot\frac{\omega\mathbf{E}\cdot\mathbf{E}}{U} \quad (1)$$

where $\mathbf{S}$ is the electromagnetic energy flux density, U is the local electromagnetic energy density, $\mathbf{E}$ is the electromagnetic field, $\mathbf{H}$ is the magnetic field, $\varepsilon_{\mathbf{k}}$ is the $\mathbf{k}$-dependent permittivity, and $\mu_{\mathbf{k}}$ is the $\mathbf{k}$-dependent permeability. In general, $\varepsilon_{\mathbf{k}}$ and $\mu_{\mathbf{k}}$ are functions of wave vector $\mathbf{k}$ and, as is well known [5], the group velocity $\mathbf{v}_g$ defined by Eq. (1) is not the same as energy velocity $\mathbf{v}_S = \mathbf{S}/U$. This is especially important in some dielectric structures that exhibit highly non-linear dispersive effects. Since electromagnetic energy flow is the physical quantity of interest, we will be concerned with calculating energy velocity $\mathbf{v}_S$ rather than group velocity $\mathbf{v}_g$.

Rather than use the popular finite difference time domain (FDTD) method [6] which is very compute intensive, we calculate $\mathbf{v}_S$ using the computationally more efficient scattering matrix method [7,8]. This approach exploits the symmetry associated with each scattering center to reduce the computation effort. For one-dimensional dielectric slabs, the propagation modes are

* Corresponding author. Tel.: +1-213-740-7318; fax: +1-213-740-9280.
E-mail address: alevi@usc.edu (A.F.J. Levi).

0038-1101/03/$ - see front matter
doi:10.1016/S0038-1101(03)00010-8

just plane waves. We use this scattering matrix approach to evaluate impedance matching and provide insight into the problem of efficient electromagnetic wave coupling to a finite PC. Our prototype device is a series of N dielectric layer pairs with index of refraction n_1 and n_2 and thickness d_1 and d_2 respectively such that $d_1 + d_2 = \Lambda$ and $d_{1,2} = \lambda/4n_{1,2}$, where λ is the incident wavelength in free space. The basic geometry showing dielectric layers stacked in the z direction is illustrated in Fig. 1(a).

Net flow of electromagnetic energy is an average of the scattered electromagnetic wave propagating inside the PC region. Since energy flow is the important physical quantity that will guide device design, we start by calculating the time averaged energy density

$$U = \tfrac{1}{4}\left(\varepsilon|\mathbf{E}(x,z)|^2 + \mu|\mathbf{H}(x,z)|^2\right) \tag{2}$$

and time averaged energy flow $\mathbf{S}_x$ and $\mathbf{S}_z$ in the x and z direction respectively.

$$\mathbf{S}_x = \tfrac{1}{2}\mathrm{Re}(\mathbf{E}_y(x,z) \times \mathbf{H}_z(x,z)) \tag{3}$$

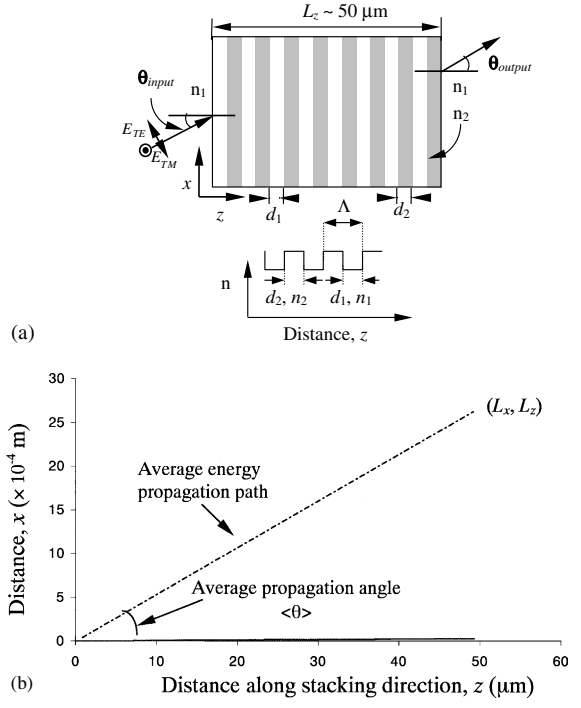

Fig. 1. (a) Geometry showing light incident at angle θ_{input} on a dielectric stack with refractive index n_1 and n_2. (b) The average propagation path of an electromagnetic wave in the periodic structure with $n_1 = 1.5$, $n_2 = 1.65$ and $d_1 = 0.258$ μm, $d_2 = 0.235$ μm. The length of one period is $d_1 + d_2 = \Lambda = 0.493$ μm. The average propagation angle is calculated by joining the incident and exit points. The wavelength of the light in free space is $\lambda = 1611.2$ nm.

$$\mathbf{S}_z = \tfrac{1}{2}\mathrm{Re}(-\mathbf{E}_y(x,z) \times \mathbf{H}_x(x,z)) \tag{4}$$

The energy velocity in the x direction is

$$\mathbf{v}_{\mathbf{S}_x}(z) = \frac{\mathbf{S}_x}{U} \tag{5}$$

and in the dielectric stacking direction z is

$$\mathbf{v}_{\mathbf{S}_z}(z) = \frac{\mathbf{S}_z}{U} \tag{6}$$

The average energy propagation path is determined by integrating the energy velocity. We choose to define the average propagation angle $\langle\theta\rangle$ by joining the incident point ($x = 0$, $z = 0$) and exit point ($x = L_x$, $z = L_z$) of the average energy propagation path in the dielectric structure such that

$$\langle\theta\rangle = \arctan\left(\frac{L_x}{L_z}\right) \tag{7}$$

The energy velocity is evaluated in each layer using the transmission and reflection coefficients obtained via the scattering matrix method. The energy propagation path is determined by integrating the energy velocity with respect to time. A representative energy propagation path and average propagation angle calculated using this method is plotted in Fig. 1(b).

A basic assumption of the scattering matrix calculation is that the beam size of the electromagnetic wave is large and energy flow is the average of the scattered electromagnetic wavelets in the structure. When wavelength is near the band-edge, the propagation path deviates greatly from a simple straight-line average propagation path (Fig. 1(b)). This is a signature of the presence of resonant modes in the finite-sized structure.

2. Resonant and anti-resonant propagation

In a one-dimensional periodic dielectric structure photons are scattered between the dielectric layers and the reflection strength at the interface depends on the refractive index difference of the dielectric pairs. When the scattered phases of the electromagnetic wave add up constructively, photons exit the structure with 100% transmission and resonant propagation takes place. When the phases add up destructively, the reflection is large and this is called anti-resonant propagation. The wavelength corresponding to resonant and anti-resonant propagation may be determined from the nulls and peaks (or reflection lobes) in the reflection spectrum. Fig. 2(a) is the typical reflection spectrum of 100 pairs of periodic dielectric structure, with $n_1 = 1.5$, $n_2 = 1.65$ and $d_1 = 0.258$ μm, $d_2 = 0.235$ μm. The length of one period is $\Lambda = 0.493$ μm. The figure shows the wavelength of the band-edge lobes and nulls in the reflection spectrum. Fig. 2(b) shows the average plane wave energy propagation

path for 15° off-normal angle incident on the dielectric structure shown in Fig. 2(a) for the indicated values of wavelength. The dispersion angle is largest for the first null in the reflection spectrum.

Resonant propagation occurs when the incident wavelength is close to the nulls of the reflection spectrum. The formation of a resonant energy distribution within the dielectric structure causes energy velocity along the stacking direction to slow down with increasing penetration into the dielectric structure. The velocity reaches a minimum value at the peak of the energy distribution and increases to its phase velocity at the input and exit of the dielectric structure. Whenever there is a resonant energy density build-up, photons are reflected back and forth in that region, and net energy velocity along the stacking direction is reduced. Energy velocity perpendicular to the stacking direction fluctuates between layers. When energy density is small, the fluctuation is large. When the energy density is large, the difference in the energy velocity is small. Fig. 3 shows the energy velocity for the first null (resonance) of the reflection spectrum.

For anti-resonant propagation (peaks in the reflection spectrum), the scattering phases add up destructively

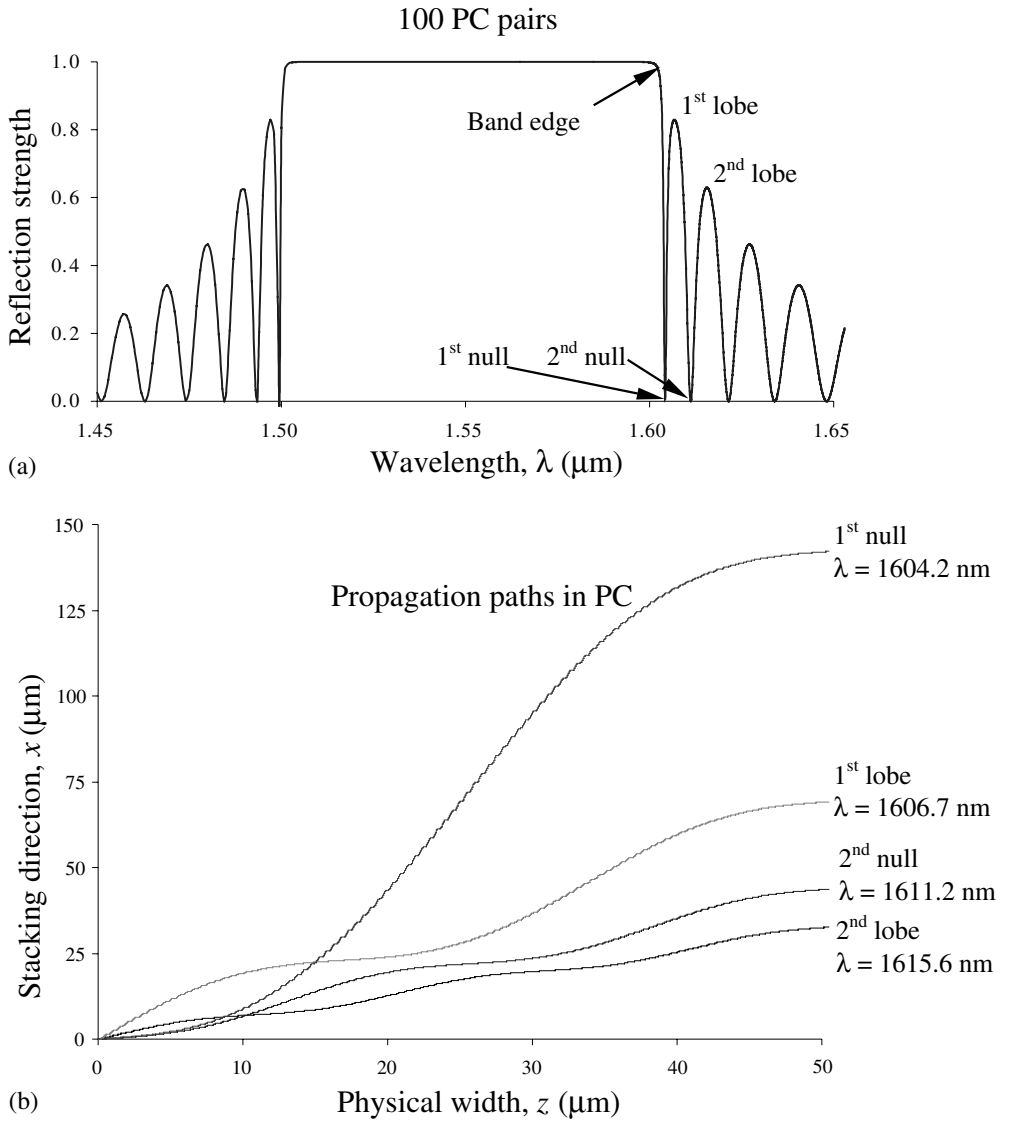

Fig. 2. (a) Reflection spectrum of 100 pairs of periodic dielectric structure, with $n_1 = 1.5$, $n_2 = 1.65$ and $d_1 = 0.258$ μm, $d_2 = 0.235$ μm. The length of one period is $\Lambda = 0.493$ μm. (b) Average propagation path for beams incident with 15° angle at different wavelengths. The dispersion angle is the largest for the first null in the reflection spectrum.

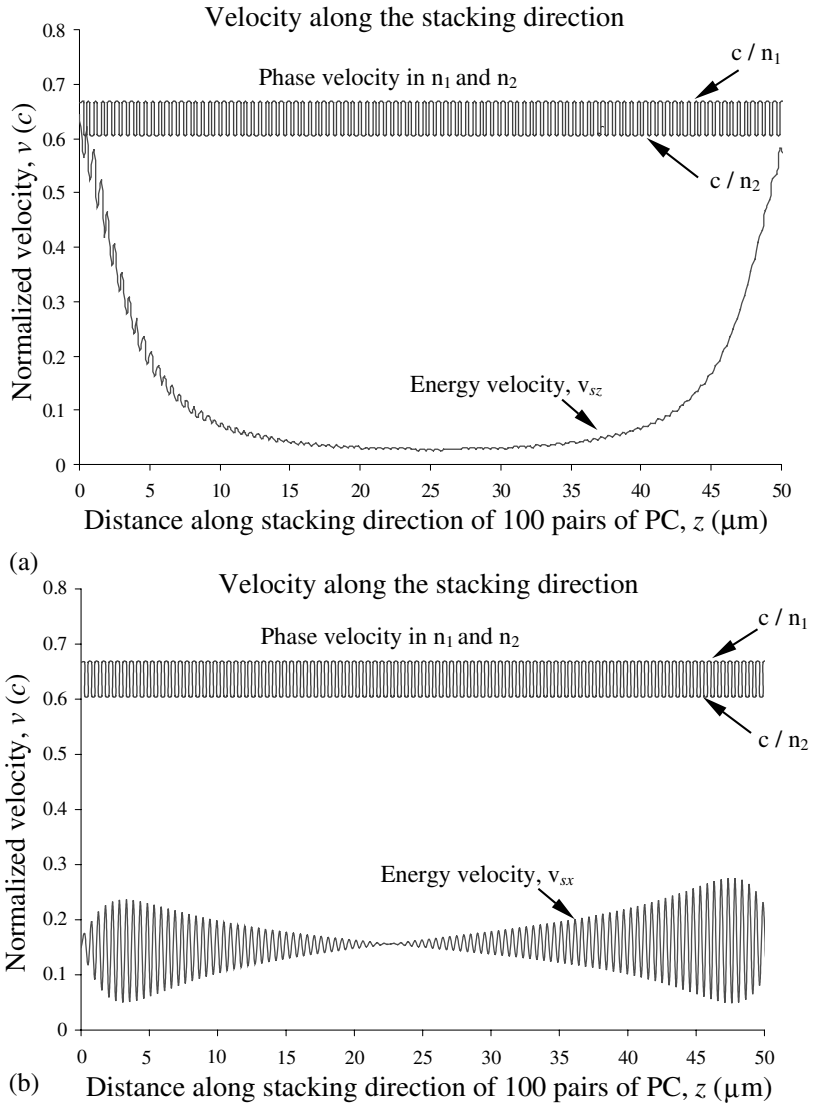

Fig. 3. (a) Energy velocity of the first null in Fig. 2 along the stacking direction in the same dielectric structure as Fig. 2. (b) Energy velocity of the first null in Fig. 2 perpendicular to the stacking direction in the dielectric structure.

and the energy density reaches a maximum at the incident surface. As the electromagnetic wave propagates through the dielectric structure, the energy density oscillates with nodes indicating which anti-resonant peak it is sitting at from the band-gap. The electromagnetic wave exits the structure with minimum energy density and a limited amount of light is transmitted. As the beam exits the dielectric structure, the energy velocity along the stacking direction approaches the phase velocity.

Wherever the scattered phases add up constructively, there will be a large energy density build-up inside the PC, the energy flow is slowed down along the stacking direction and this influences the electromagnetic propagation path. When the wavelength is detuned from resonant nulls in the reflection spectrum, the reflection is strong with the formation of an anti-resonant energy distribution in the structure.

For electromagnetic energy propagation at the band-edge, the difference of the energy velocity along and perpendicular to the stacking direction is large, and the dispersion angle is approximately 90° (Fig. 4).

3. Far from band-edge transmission

When the optical wavelength is far away from the band-edge, the resonant and anti-resonant modes no

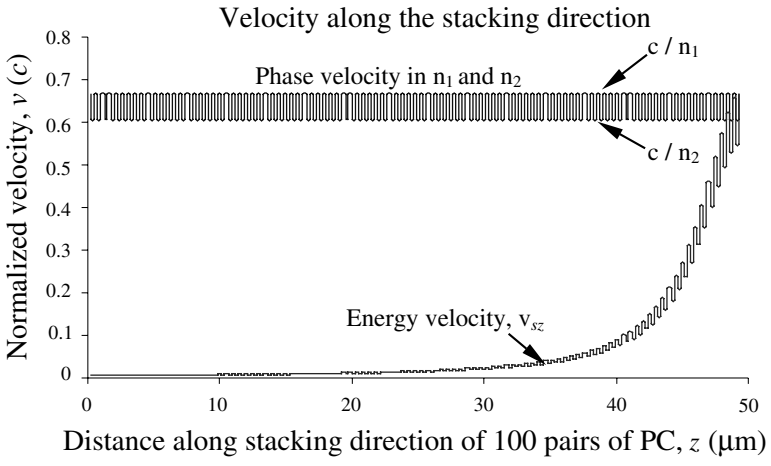

(a)

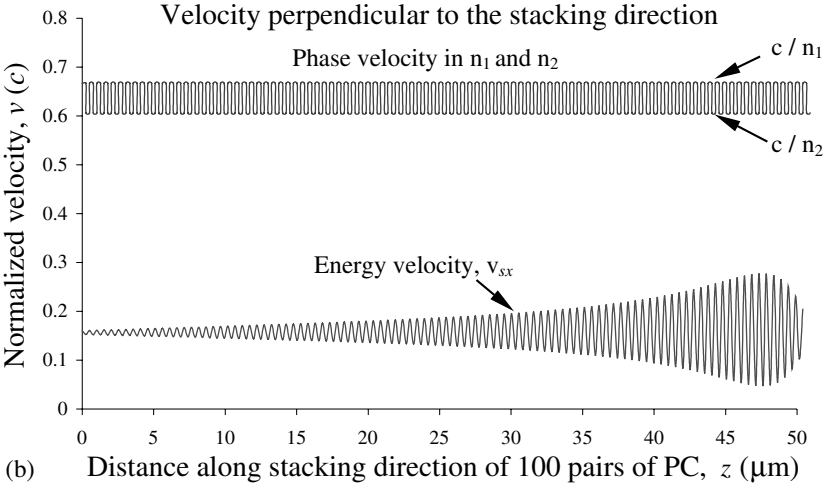

(b)

Fig. 4. (a) Energy velocity along the stacking direction in the 100 pairs periodic dielectric structure with $n_1 = 1.5$, $n_2 = 1.65$ and $d_1 = 0.258$ μm, $d_2 = 0.235$ μm. The length of one period is $\Lambda = 0.493$ μm and incident angle = 15°. The incident wavelength is near the band-edge. (b) Energy velocity perpendicular to the stacking direction in the dielectric structure at the same wavelength for the same structure.

longer influence the propagation path. The effective dielectric constant [9] is

$$\frac{1}{\varepsilon_{\text{eff}}} = \frac{1}{\Lambda}\left(\frac{d_1}{\varepsilon_1} + \frac{d_2}{\varepsilon_2}\right) \tag{8}$$

For the periodic structure with dielectric constant $n_1 = 1.5$, $n_2 = 1.65$, $d_1 = 0.258$ μm, $d_2 = 0.235$ μm, and $n_{\text{eff}} = \sqrt{\varepsilon_{\text{eff}}} = 1.566$. According to Snell's law, $n_1 \sin\theta_1 = n_{\text{eff}} \sin\theta_{\text{prop}}$ so for an incident angle $\theta_1 = 15°$, the propagation angle is $\theta_{\text{prop}} = 14.35$. We obtain a similar result using the scattering matrix calculation. In Fig. 5(a) reflection spectrum is calculated for 100 pairs of PC with $n_1 = 1.5$, $n_2 = 1.65$ and $d_1 = 0.258$ μm, $d_2 = 0.235$ μm. The length of one period is $\Lambda = 0.493$ μm and incident angle = 15°, the dot indicates the wavelength $\lambda = 1980$ nm where the propagation path is calculated. Fig. 5(b) shows that the average propagation angle for wavelength far from band-edge approaches the same value as obtained from Snell's law for the effective medium. Very far from band-edge, the refraction angle obtained using Snell's law and an effective medium is the same as the calculated average energy propagation angle.

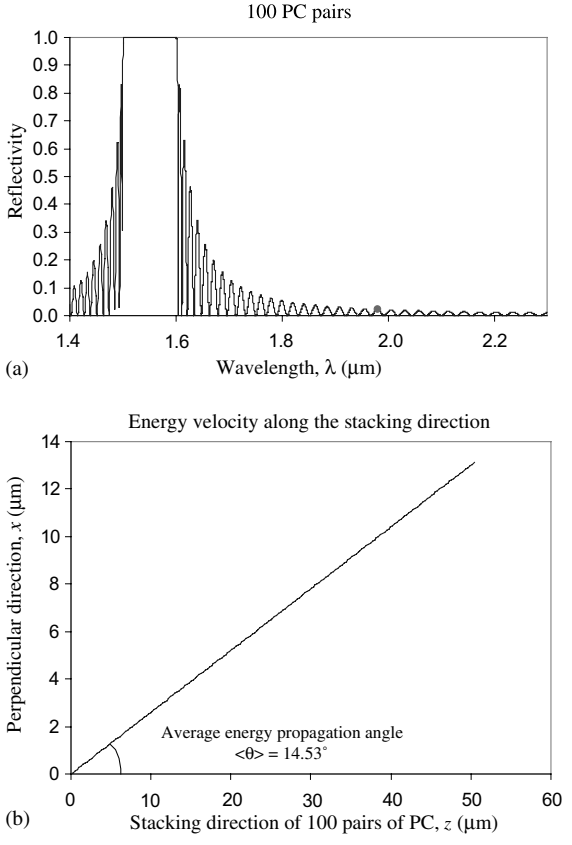

Fig. 5. (a) Reflection spectrum of 100 pairs of PC with $n_1 = 1.5$, $n_2 = 1.65$ and $d_1 = 0.258$ μm, $d_2 = 0.235$ μm. The length of one period is $\Lambda = 0.493$ μm and incident angle $= 15°$, the red dot is at the wavelength where the propagation path is calculated. (b) The average propagation angle (14.53°) for wavelength $\lambda = 1980$ nm approaches the same value obtained from Snell's law for the effective medium (14.35°).

4. Adiabatic impedance matching regime

Since the Bloch modes in the PC are of different symmetry from the propagation modes of a uniform media, by breaking the symmetry of the PC it should be possible to efficiently couple the propagation modes of a uniform media to the PC modes. In this way we can make use of the highly dispersive Bloch modes near the band-edge while simultaneously keeping reflection at a low value. In a simplistic approach, one may either vary the duty cycle of the layer thickness or vary the composition of the material in each layer. In this paper, we adopt the layer thickness grading method.

An impedance matching dielectric structure can reduce the anti-resonant peaks near the band-edge and enhance coupling efficiency. The issue is to find profile functions that maintain a well-defined (sharp) band-edge while simultaneously giving an acceptably low insertion loss over a range of wavelengths.

To illustrate the effect of grading to achieve impedance matching we consider a number of approaches that illustrate the physics involved. The grading region can be described by a normalized strength function. The formula we use for exponential grading is

$$f(i) = d_2 \exp\left(\frac{i-N}{mi}\right) \tag{9}$$

where N is the number of the grading pairs, d_2 is the thickness of the dielectric layer 2 in the structure, i is the layer pair index, and m is a grading sharpness factor. The formula we use for Gaussian grading is

$$f(i) = d_2 \exp\left(-\frac{(1-i/N)^2}{\sigma^2}\right) \tag{10}$$

where N is the number of the grading pairs, σ is the grading smoothness factor. The formula we use for our modified exponential grading is

$$f(i) = d_2 \exp\left(\frac{i-N}{mi}\right)\left(1 - \frac{i-N}{mi}\exp\left(-\frac{(1-i/N)^2}{\sigma^2}\right)\right) \tag{11}$$

where N is the number of the grading pairs, σ is the grading smoothness factor, m is the grading sharpness factor.

By comparing propagation angle dispersion spectrum and reflection spectrum for the Gaussian grading and modified exponential grading scheme, we can obtain some insights into grading profile design. The Gaussian profile provides a smooth function increasing from very small duty cycle to unity duty cycle. In our calculation, σ is 33% of the total grading region length, which, when the number of impedance matching pairs is large, results in a good adiabatic coupling approximation [10]. The difference between the Gaussian grading profile and the modified exponential grading profile lies in the grading steepness in the initial grading pairs as shown in Fig. 6.

A typical reflection spectrum after adding grading pairs is shown in Fig. 7. In this particular case, the reflection spectrum is computed for 100 PC pairs and 50 pairs of exponential grading pairs ($m = 5$) at each side of the PC. The refractive index for each material is $n_1 = 1.5$, $n_2 = 1.65$ and the thickness of each material layer is $d_1 = 0.258$ μm, $d_2 = 0.235$ μm respectively. The length of one period is $d_1 + d_2 = \Lambda = 0.493$ μm. The strong reflection at the first and subsequent lobes on the long wavelength side of the band-gap is significantly reduced.

A key issue to address in a simple transmission mode super-prism device is minimization of reflectivity near the optical band-gap to access the large band-edge dispersion. At the same time, the impedance matching structure used should not significantly change the near band-edge dispersion. Of the grading functions consid-

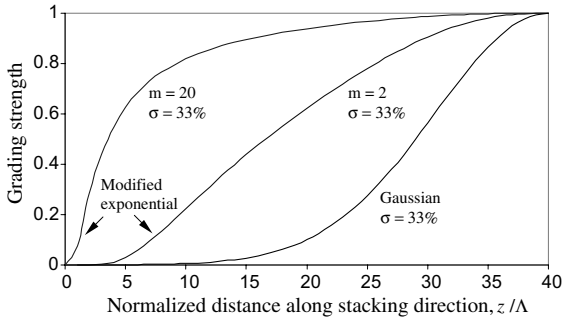

Fig. 6. (a) Grading profile of the modified exponential function for sharpness factor $m = 20$ and $m = 2$, $\sigma = 33\%$. When m is larger, the initial slope of increase is larger. (b) Grading profile of the Gaussian function with $\sigma = 33\%$. The initial grading sharpness is very small compared to the modified exponential grading.

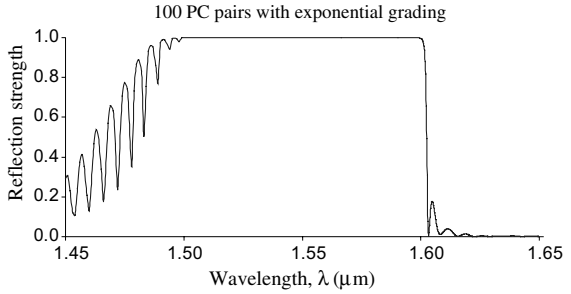

Fig. 7. Reflection spectrum of 100 pairs of PC and 50 pairs of exponential grading pairs ($m = 5$) at each side of the PC. The refractive index for each material is $n_1 = 1.5$, $n_2 = 1.65$ and the thickness of each material layer is $d_1 = 0.258$ μm, $d_2 = 0.235$ μm respectively. The total length of one period is $\Lambda = 0.493$ μm. The strong reflection at the first peak is significantly reduced, but the dispersion angle is also decreased.

ered here, the modified exponential (Eq. (11)) gives the best results.

In Fig. 8(a), the grading steepness of the modified exponential grading is much greater than Gaussian

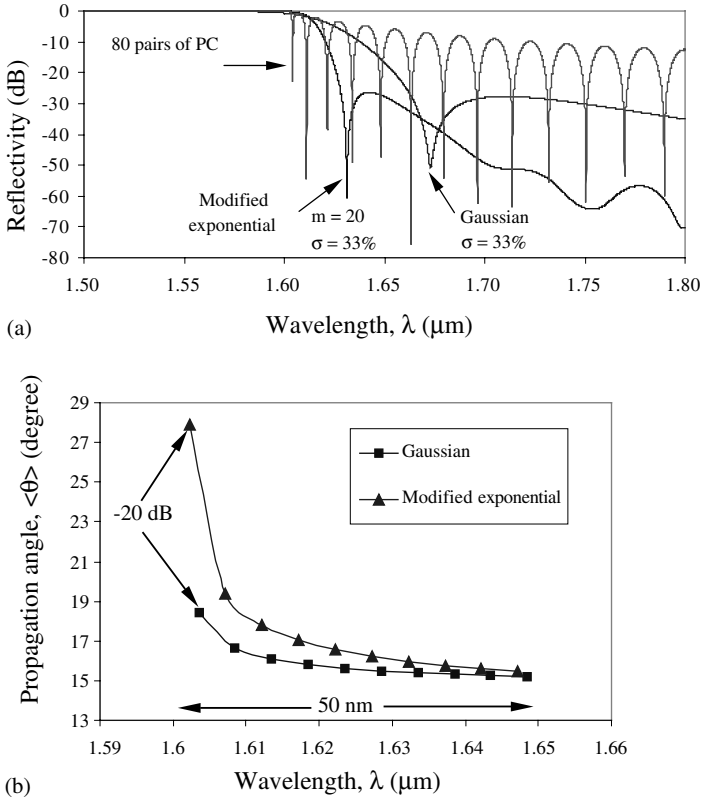

Fig. 8. (a) Reflection spectrum of 80 pairs of PC, and 40 impedance matching pairs of the Gaussian and modified exponential grading with m and σ parameters shown. The refractive index for each material is $n_1 = 1.5$, $n_2 = 1.65$ and the thickness of each material layer is $d_1 = 0.258$ μm, $d_2 = 0.235$ μm respectively. The total length of one period is $\Lambda = 0.493$ μm. The modified exponential grading reached the −20 dB point faster than the Gaussian grading. (b) The angle dispersion of the modified exponential grading varies greater than the Gaussian grading over the 50 nm wavelength range.

grading near the edge of the incident region. As a result, in the reflection spectrum, the reflectivity decreases rapidly at the band-edge and reaches −20 dB closer to the band-edge compared to the Gaussian function. For the Gaussian function, the reflection spectrum is smeared at the band-edge. In Fig. 8(b), the modified exponential grading provides larger angle dispersion than the Gaussian grading. The angle dispersion of the modified exponential grading varies near 15° over a 50 nm wavelength range. The angle dispersion in this 50 nm wavelength range is non-linear. For the modified exponential grading, at the wavelength with −20 dB reflectivity, the angle dispersion varies around 10° over the initial 10 nm wavelength, and then changes only around 5° in the next 40 nm. To access more of the highly non-linear dispersion further one could start from the wavelength with −10 dB reflectivity as shown in Fig. 9. But since the reflection spectrum of the modified exponential grading drops down so quickly at the band-edge, the improvement for the modified exponential grading is only around 2 nm closer to the highly non-linear band-edge.

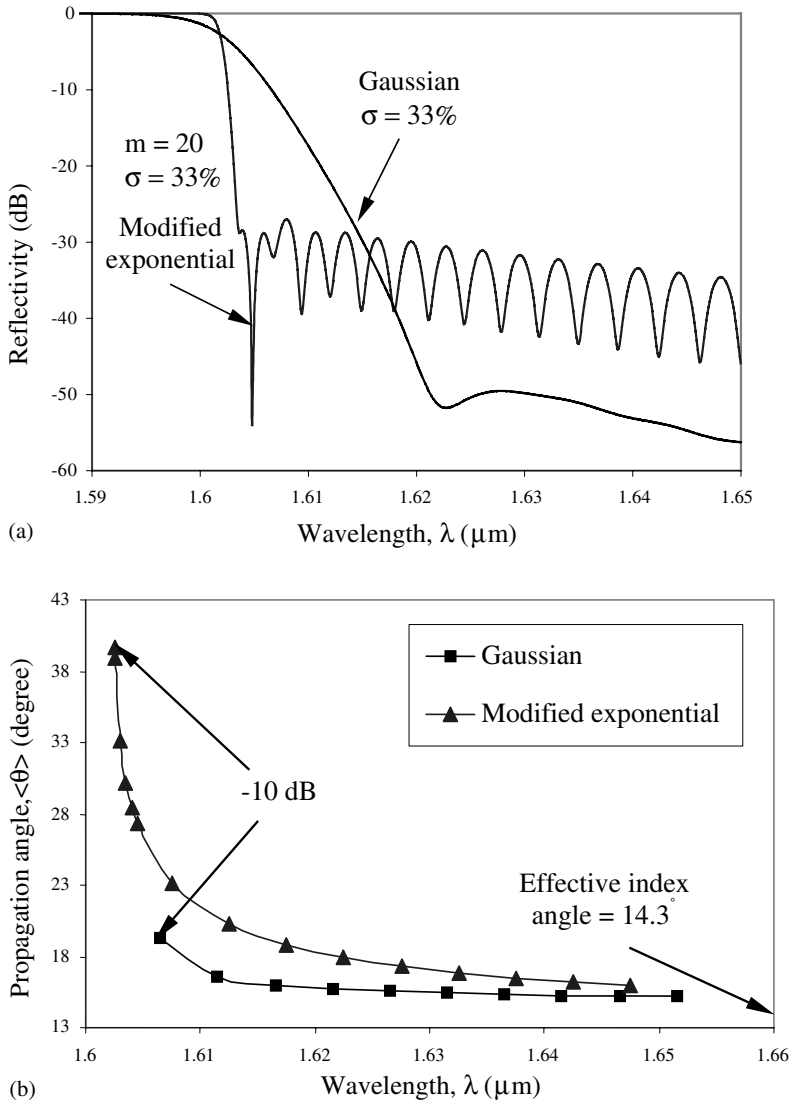

Fig. 9. (a) Reflection spectrum of 40 impedance matching pairs of the Gaussian and modified exponential grading for $n_1 = 1.5$, $n_2 = 1.65$ and the thickness of each material layer is $d_1 = 0.258$ μm, $d_2 = 0.235$ μm respectively. The total length of one period is $\Lambda = 0.493$ μm. (b) The angle dispersion curve starts from the wavelength with −10 dB insertion loss instead of −20 dB loss. The dispersion curve is highly non-linear near the band-edge, and the refraction angle by effective medium theory is 14.3°.

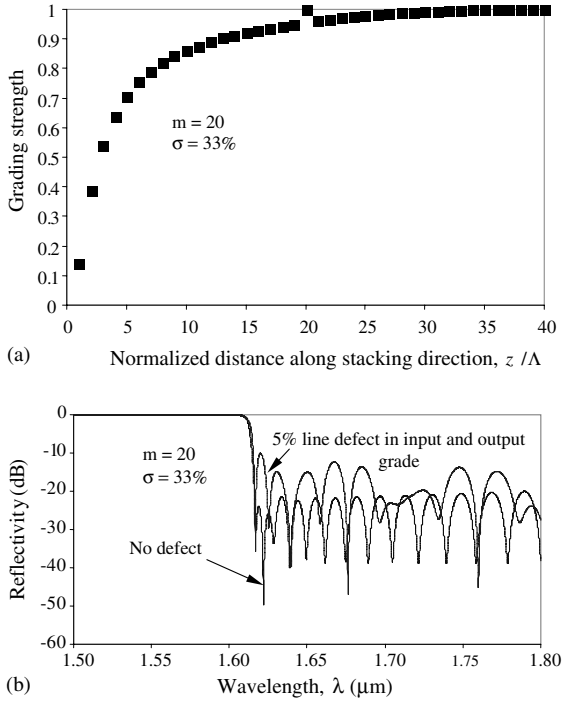

Fig. 10. (a) The grading profile of 40 dielectric pairs at each side of a PC consisting of one dielectric pair, with a 5% thickness line defect in the dielectric structure, with grading parameters $m = 20$, and $\sigma = 33\%$. The refractive index is $n_1 = 1.5$, $n_2 = 1.65$ and the thickness of each material layer is $d_1 = 0.258$ μm, $d_2 = 0.235$ μm respectively. The total length of one period is $\Lambda = 0.493$ μm. (b) The reflection spectrum for grading profile with and without the line defect in the input and output grading regions. Reflection is significantly enhanced by the presence of the 5% line defect.

5. Fabrication tolerances

The geometry of the impedance matching region is limited by current nano-fabrication techniques. Surface roughness of the dielectric and average thickness variation of a dielectric layer in the impedance matching region can dramatically change optical mode matching properties. An approximately 5% change in the thickness of one dielectric layer in the grading structure (Fig. 10(a)) changes optical reflectivity by more than 10 dB near the band-edge (Fig. 10(b)). When fabricating the dielectric layers near the PC region, the scattering strength due to the defect layer is much larger than it is at the non-PC incident or exit regions of the impedance matching structure. Defects in high scattering strength regions ($f(i) \sim 1$) cause larger changes in reflection than low scattering strength regions ($f(i) \sim 0$). Surface roughness and stochastic variation in the thickness of dielectric layers also changes reflectivity. FDTD calculations show that root-mean-squared variations of 10 nm for typical dielectric structures we have been considering results in band-edge broadening and reduced super-prism dispersion.

6. Conclusion

By breaking the symmetry of a PC it is possible to efficiently couple light into a nano-scale dielectric structure. Optical energy flow in the beam-pointing direction is the physical quantity of interest. A periodic dielectric stack is not necessary to obtain significant angle dispersion, broken symmetry structures can also act as super-prisms. The challenge is to simultaneously achieve low insertion loss (<1%) for incident wavelengths $\lambda = 1550$ nm with a relatively small device size (<500 μm on a side) which is insensitive to 10-nm-sized defects. A modified exponential impedance matching function can be used to couple light over a large range of incident wavelengths with small reflectivity. This approach opens up the possibility of practical applications that make use of the highly dispersive properties of non-periodic dielectric structures for transmission mode devices.

References

[1] Ohtaka K. Energy band of photons and low energy photon diffraction. Phys Rev B 1979;19:5057–67.
[2] Kosaka H, Kawashima T, Tomita A, Notomi M, Tamamura T, Sato T, et al. Superprism phenomena in photonic crystals. Phys Rev B 1998;58:R10096–9.
[3] Lin SY, Hietala M, Wang L, Jones ED. Highly dispersive photonic band-gap prism. Opt Lett 1996;21:1771–3.
[4] Zengerle R. Light propagation in singly and doubly periodic planar waveguides. J Mod Opt 1987;34:1589–617.
[5] Brillouin L. Wave propagation and group velocity. New York: Academic Press; 1960.
[6] Yee KS. Numerical solution of initial boundary value problem involving Maxwell's equations in isotropic media. IEEE Trans Antennas Propagat 1966;AP-14:302–7.
[7] Gralak B, Enoch S, Tayeb G. Anomalous refractive properties of photonic crystals. JOSA 2000;A17:1012–20.
[8] Yeh P. Optical waves in layered media. New York: Wiley & Sons; 1988.
[9] Scaife B. Principles of dielectrics. Oxford: Oxford Science Publications; 1998.
[10] Russel P, Birks TA. Hamiltonian optics of nonuniform photonic crystals. J Lightwave Technol 1999;17:1982–8.